Subcompact Hydrogen Maser Atomic Clocks

HARRY T. M. WANG

Invited Paper

Recent progress in compact hydrogen maser atomic frequency standards or clocks is reviewed. After a brief description of the principle of a hydrogen maser, the techniques employed to realize high-performance compact hydrogen masers are discussed. Two approaches in compact hydrogen maser design are presented. 1) Active or atomic resonance sustained maser oscillation. The design employs cavity Q enhancement to overcome the intrinsic higher losses in a compact cavity. The versatility of the cavity design enabled masers of various sizes to be realized. The complete package for the smallest oscillating compact maser measures 17.8 × 30.5 × 43.2 cm, weighs 19.5 kg, and has a measured stability of 4.14×10^{-14} for an averaging time $\tau = 400$ s, with a $\tau^{-1/2}$ dependence for $\tau < 10^5$ s. 2) Passive maser. The design employs the atomic resonance as a narrow-bandpass amplifier. Using a dielectric loaded cavity, a package size of 26.7 × 66 × 45.5 cm, weighing 30 kg, with a stability of $1.0\text{–}3.0 \times 10^{-12} \tau^{-1/2}$, for $1 < \tau < 10^5$ s, has been attained. Compact masers of both designs have demonstrated frequency drift rates of 1×10^{-15} per day or less.

I. Introduction

In this paper, a review of recent progress in compact hydrogen maser atomic frequency standards or clocks is given. The objective and challenge of compact maser development is a device in a compact package without unacceptably large sacrifice in the stability performance characteristics of a hydrogen maser. An indication of the progress in this endeavor is provided by a Q-enhanced subcompact hydrogen maser oscillator, CHYMNS-IIIb, developed at Hughes Research Laboratories. The physics unit of the maser measures only 15.5 cm square by 37 cm long and weighs 10.2 kg. Compared to a full-size hydrogen maser, these parameters represent approximately 16-fold reductions in size and 30-fold in weight. The complete maser is housed in a rack-mountable package 17.8 × 30.5 × 43.2 cm, which is about the size of a high-performance commercial cesium-beam frequency standard. With a measured stability of 4.14×10^{-14} for an averaging time $\tau = 400$ s, and varying as $\tau^{-1/2}$ for $\tau < 10^5$ s, the maser is more stable than the commercial cesium standard by at least a factor of 4.

The unsurpassed short-term stability performance of the hydrogen maser has been employed in critical timing applications. Hydrogen masers provide timing reference for the Deep Space Network of the National Astronautics and Space Administration (NASA) [1]. At the U.S. Naval Observatory in Washington, DC, which maintains standard time for the Department of Defense and, indeed, for the United States (this responsibility is coshared with NIST, formerly NBS), a hydrogen maser is a critical link in a state-of-the-art timing reference system employing a trapped mercury ion device [2]. A hydrogen maser is the device of choice as the precise timing reference for very long baseline interferometry (VLBI) investigations [3]. However, the bulkiness of the conventional maser is a distinct drawback in some system considerations. A compact and portable device would be very attractive to applications that need the stability and accuracy characteristics, but which cannot tolerate the size and weight of a conventional hydrogen maser.

Development of the compact hydrogen maser has been supported by the U.S. Naval Research Laboratory [4]. The program is a response to the need for an extremely stable satellite-borne atomic clock for the space-based radio navigation system, the Navstar Global Positioning System (GPS), which is being developed by the Department of Defense [5]. The space segment of GPS will contain 21 atomic clocks carrying satellites in six orbital planes plus three in-orbit spares. When fully operational in the 1990s, at least four satellites will be visible at any point on the surface of the earth at any time. The system determines position by triangulation, using the time of arrival of radio signals from three different satellites. (A fourth satellite signal will provide time synchronization if the receiver does not have an adequate timing reference of its own.) Time and distance are related by the speed of light, and a timing error of 1 ns translates into a position error of 0.3 m (approximately 1 ft) for an orthogonal set of satellites. A number of factors (such as clock stability, uncertainties in satellite ephemeris, ionospheric propagational delays, geometrical dilution of precision) contribute to the precision of a satellite-based navigation system. The clock is nevertheless a critical component of the system. A good clock will have proportionally small contribution to the system error budget. Thus if the clock contribution to the position error is to be kept to within a desirable value of 1.5 m [4], then the clocks have to be maintained to within 5 ns. The required clock stability should be better than 6×10^{-14} over a 24-h period [6]. This stability requirement is difficult for spaceborne cesium and rubidium clocks to meet [7]. Operationally, poor clock stability requires constant tracking and frequent updates to

Manuscript received July 25, 1988; revised March 20, 1989.

The author is with Hughes Research Laboratories, Malibu, CA 90265, USA.

IEEE Log Number 8928441.

0018-9219/89/0700-0982$01.00 © 1989 IEEE

maintain system accuracy. By the same token, the higher stability of a maser clock means that the required system update is much less frequent. In addition to operational economics, the better clock will provide margins for potential upgrade of system performance. Even in the current developmental stage, GPS has demonstrated a significant impact on precise time transfer and synchronization of remotely located clocks [8]. Using GPS, time transfer has been demonstrated to be more precise [9] and more economical than traveling clocks, and the technique is also more universally applicable. The contribution of GPS in this area is bound to grow in importance in parallel with the growth in the application of precise time and time interval in science, technology, and industry. Technological advances will demand ever more precise time and frequency reference standards for calibration and measurements. Some well-known applications of precise time are in high-volume data transmission, in secured communication using time division multiplexing, and in the operation of modern telephone and broadcast television networks. Precise time has also been successfully exploited in such diverse areas as surveying for offshore exploration and drilling [10] and in power utilities for locating faults in transmission lines [11].

In the remainder of the paper we first briefly describe the principle of the hydrogen maser. The approaches to reducing the size and weight of the device and their effect on the performance of a compact maser are discussed. Two specific compact maser designs and their characteristics are reviewed. One design, the Q-enhanced maser oscillator, employs a hydrogen resonance to sustain oscillation in a microwave cavity whose quality factor is enhanced electronically. The other design, the passive maser, uses the atomic resonance as a narrow bandpass amplifier. A brief discussion on the state-of-the-art development in atomic frequency standards is given in the concluding section.

II. Principle of the Atomic Hydrogen Maser

The atomic hydrogen maser was invented in 1960 by D. Kleppner and N. F. Ramsey. It is an atomic beam storage device whose stability and accuracy as a reference frequency standard or atomic clock is well known, and the theory and techniques of the device have been described in detail [12], [13]. For the sake of completeness, we give here a brief description of the device. Our discussion will emphasize the effect of size reduction on the performance of the maser.

The maser operates on the ($F = 1, m_F = 0 \rightarrow F = 0, m_F = 0$) field-independent hyperfine transition in the ground-state hydrogen atom at 1.42 GHz. A schematic diagram of the device is shown in Fig. 1. Hydrogen atoms, created by an RF discharge, are formed into a beam. After passing through a state selector magnet, atoms in the upper maser transition level are deflected into the Teflon-coated storage bulb located in a low-loss TE_{011} mode resonant microwave cavity. The atoms are stimulated to radiate by the axial component of the cavity microwave magnetic field. If the power radiated by the atoms is sufficient to overcome the losses in the cavity, then a sustained maser oscillation is obtained. Since the confined radiating atom has near zero net velocity, there is negligible linear Doppler effect. The long interaction time between the radiating atom and the coherent

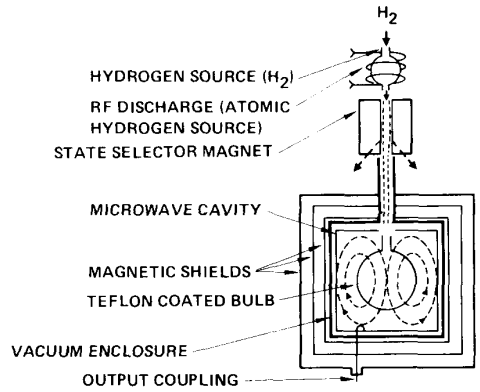

Fig. 1. Schematic of hydrogen maser.

cavity electromagnetic field produces a resonant signal of very high spectral purity. For a conventional maser with a 17-cm-diameter storage bulb, the atomic resonant linewidth is typically about 0.7 Hz, or an atomic line Q of 2×10^9. The maser oscillation signal is processed in a coherent heterodyne receiver and is used to phase-lock a voltage-controlled crystal oscillator (VCXO), which provides the system output.

In free space, the atomic transition frequency is invariant. However, several physical processes perturb the atoms in a maser. The most significant ones are summarized in Table 1. The operational offsets shown are for the indicated perturbations in a subcompact maser with a storage bulb of diameter $D = 5$ cm operating at a temperature $T = 313$ K and an applied magnetic field $H_0 = 250\ \mu$G. A consequence of confining the restless atoms is that they will collide with the container wall, and the collisions perturb the atomic energy levels. The phase shift in the atomic wave function for each wall collision, and hence the wall collision frequency shift coefficient W, depends on the wall-coating material and is also a function of the surface condition, including temperature. The temperature effect is measured with respect to a reference temperature T_0 and is characterized by a coefficient α_W. Precise measurement of the wall collision induced frequency shift is complicated by the necessity to change surfaces or storage bulbs for comparison [14]. The estimated wall shift shown in Table 1 is for a storage bulb coated with FEP-120 Teflon, which is the most commonly used coating material. The atom will maintain its quantum state for approximately 10^5 bounces against a properly coated surface. Since the relaxation is propor-

Table 1 Perturbations to Maser Oscillation Frequency

Perturbation	Equation	Offset
Wall collision	$\delta\omega_w = W\frac{1 + \alpha_w(T - T_0)}{D}$	5×10^{-11}
Cavity and spin-exchange pulling	$\delta\omega_c = \frac{Q_c(\omega_c - \omega_0) - \alpha/Q_c}{Q_a}$	0*
Magnetic field	$\delta\omega_H = 2.75 \times 10^3 H_0^2$	1.2×10^{-13}
Second-order Doppler	$\delta\omega_D = \frac{-3kT}{2mc^2}\omega$	-4.3×10^{-11}

*Cavity spin-exchange tuned and no higher order effects.

tional to the rate of collision with the wall, it is more severe in a compact maser with a small storage bulb. In the CHYMNS-IIIb subcompact maser with a 5-cm-diameter storage bulb, an atomic line Q of 7×10^8 has been observed. Compared to the line Q for a full-size maser, this is in approximate linear proportion to the diameter of the storage bulb. Although the estimated wall collision frequency shift is also higher, it is expected to be constant in time and should have little effect on the stability of the maser. To appreciate the effectiveness of the storage technique in reducing the maser resonant linewidth, consider a cesium-beam frequency standard. The atomic resonant linewidth is proportional to the inverse of the transit time through the Ramsey cavity [15]. Thus even for the heavy cesium atoms with relatively low thermal velocities (about 12 times slower than hydrogen atoms at the same temperature), to obtain a fractional linewidth comparable to that obtained in a CHYMNS-III subcompact hydrogen maser will require a beam tube 6 m long.

The radiating atoms and the microwave cavity form a pair of coupled oscillators. The drift in one will pull the frequency of the other in proportion to the ratio of their resonant linewidths. Indeed, the dominant limitation on the long-term stability of the maser had been due to drift in the cavity resonant frequency. The classical cavity design relied on thermal mechanical means to minimize the drift in the resonant frequency of the cavity. The techniques employed to reduce the size of the maser cavity also increased its sensitivity to temperature variations. This and the wall collision broadened maser resonant linewidth make an improved technique for controlling the cavity frequency a critical design requirement for a compact maser. Thus, as we will see, every compact hydrogen maser has an electronic cavity stabilization servo system. This feature, born out of necessity, has enabled the compact masers to have long-term stability as good as or better than that of a full-size maser of the conventional design. Of course, the long-term stability of the full-size maser can be improved by incorporating an electronic cavity stabilization system [16].

The relation between the maser oscillation frequency and the cavity frequency is significantly different from that between a pair of classical coupled oscillators. In the latter case, the shift in the atomic resonant frequency $\delta\omega_a$ due to an offset $\delta\omega_c = \omega_c - \omega_0$ in the cavity frequency is

$$\delta\omega_a = \frac{Q_c}{Q_a}\,\delta\omega_c \tag{1}$$

where Q_c and Q_a are cavity and atomic line Q, respectively. In the hydrogen maser, the major relaxation processes that broaden the resonant linewidth are 1) escape of the atom from storage with a time constant reflecting the geometry of the design; 2) collisions of the radiating atoms with the wall of the storage bulb; 3) transitions induced by motion through magnetic field gradients; and 4) interatomic collisions. Collisions between hydrogen atoms occur at a rate proportional to the atomic density and produce two significant effects. The collision may be strong enough to flip the electron spin of the radiating atom. This process shortens the radiative lifetime of the atom, producing a broadened resonant linewidth. For a weak collision, multiple collisions will be needed to cumulatively produce a spin flip. However, the wave function of the radiating atom will suffer a phase shift for each collision. The periodic occurrences of such collisions result in a frequency shift. These so-called spin-exchange collisions lead to a maser tuning equation which is different from Eq. (1) and, to first order, can be written as [17]

$$\delta\omega_a = \frac{Q_c\delta\omega_c - \alpha/Q_c}{Q_a} \tag{2}$$

where α is a geometric constant for a given maser. Equation (2) shows that the cavity pulling and the spin-exchange shift will compensate each other if the cavity is offset by

$$\delta\omega_{cse} = \frac{\alpha}{Q_c^2}.$$

This spin-exchange tuned cavity frequency is significant in that it makes the maser self-calibrating since the offsets due to the cavity pulling and the spin-exchange collisions compensate each other, giving a null offset. Note that for the spin-exchange tuned cavity frequency, the maser oscillation frequency is independent of the atomic linewidth, and hence of flux variations. Consequently the stability of the maser also improves. Moreover, the spin-exchange tuned condition can be determined in situ. The maser resonant linewidth is easily modulated by changing the interatomic collision rate obtained by varying the hydrogen flux. By measuring the maser oscillation frequency at two different flux levels as a function of the cavity frequency, the spin-exchange tuned cavity frequency is obtained by interpolation. The cavity frequency is typically adjusted via the bias voltage of a reactance tuner. Thus an independent measurement or calibration of the cavity is not necessary.

Equation (2) is a good approximation when higher order effects such as magnetic gradient shift [18] and hyperfine phase delay during atomic collisions [19] are neglected. These higher order effects introduce offsets which can be determined experimentally for a given maser to meet accuracy requirements. The effect on the stability of the maser is expected to be small.

Other perturbations on the maser frequency include the following. 1) Second-order Doppler shift due to changes in the atomic velocity caused by temperature variations. The light mass m of the hydrogen atom imposes a temperature stability requirement of 0.07 K to hold the second-order Doppler effect induced frequency variation within 1×10^{-14}. 2) Magnetic field dependence of the atomic energy levels and relaxation due to the motion of radiating atoms through magnetic field gradients. 3) In addition to the spin-exchange collisions between hydrogen atoms discussed, collisions with background gases may also be significant depending on the composition of the residual gases. To minimize collisional relaxation, an ultrahigh vacuum (on the order of 10^{-6} torr) is a necessity for maser operation. Designs for environmental controls to eliminate or minimize the effect of various perturbations are critical requirements in the engineering for a stable maser frequency output.

III. Maser Size Reduction

The dominant size constraint of the atomic hydrogen maser arises from the requirement of a TE_{011} mode high-Q cavity resonating at the 1.42 GHz (21-cm-wavelength) maser transition frequency to sustain maser oscillation. The first step in an attempt to reduce the size of the maser is select-

ing a compact cavity design. One technique employs metal electrodes placed inside a cylindrical cavity as loading structures [20], [21]. A 7.5-cm right cylindrical electrode loaded cavity resonating at 1.42 GHz is shown in Fig. 2. The

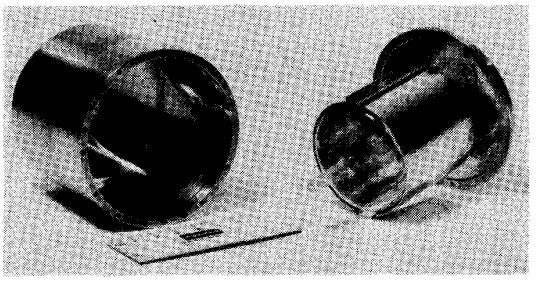

Fig. 2. 7.5-cm right cylindrical, electrode-loaded 1.42-GHz resonant cavity.

electrodes are attached to the quartz storage bulb by low-loss epoxy. The dimensions of the inductive electrodes and the capacitive gaps between them are selected to give the desired cavity resonant frequency. In addition to a reasonably high Q and a good filling factor, the design allows the flexibility of trading off the desired degree of compactness for cavity performance parameters. Indeed, compact masers have been constructed using cavities of this basic design with diameters of 15, 11, and 7.5 cm, respectively [22]. A thermally and mechanically more stable cavity for a prototype spaceborne compact maser was fabricated by plating silver film electrodes directly on the storage bulb [23]. Since losses in the cavity are dominated by the resistive losses in the electrodes, the ability to fabricate high-conductivity films is a critical requirement.

An alternate approach to reducing the size of the cavity is loading the cavity with materials of high dielectric constants and low-loss tangents. Single crystalline sapphire [24] and electrical ceramic [25] have been employed successfully. The axial portion of a cylinder of the dielectric is bored out to provide space for the storage bulb. The dielectric cylinder is either contained in an outer metal cylinder or silver plated on the outer wall to confine the electromagnetic field. Such cavities tend to be rather heavy due to the mass of the dielectric. They also have relatively high temperature coefficients dictated by that of the dielectric. Furthermore, the dimensions of the resultant cavity are determined by the properties of the dielectric, and the design does not provide flexibility in size reduction as does the electrode loading approach.

The dimensions of the vacuum vessel and the magnetic shields are constrained by the cavity design. Maser magnetic shield design and performance have been studied by Gubser *et al.* [26]. Another maser component that contributes significantly to the size and weight of the device is the vacuum pump. The continuous hydrogen flow and the ultrahigh vacuum needed for maser operation impose a pump capacity requirement proportional to the hydrogen consumption rate and the design life of the device. Until recently, the sputtering ion pump has been used exclusively on hydrogen masers because it is clean and operates without mechanical vibrations. However, it is also responsible for a good fraction of maser operational problems [27]. An alternative is to use a combination system consisting of a zirconium graphite getter and a small ion pump. Application of getter pumping to long-term operation of hydrogen masers has been studied by workers at NRL [28] and Hughes [29]. The getter offers compactness, large pumping speed, and capacity for hydrogen. Furthermore, after initial activation, it does not consume any power during operation. The small ion pump (pumping speed: 2 l/s), which is throttled to prolong pump life and improve reliability, is used to pump the small amount of nongetterable contaminants. A clean system design, including metal seals to minimize outgassing and permeation of atmospheric gases and high-vacuum processing practice, is essential for a getter-pumped maser vacuum system.

For storage of a molecular hydrogen supply, mischmetal [29] and uranium [25] hydrides have replaced the conventional pressure vessel and mechanical regulator. Furthermore, the sorption and desorption process of the hydride storage technique automatically purifies the hydrogen supply. Indeed, the hydrides have contributed to improved reliability and the small size and weight of the compact hydrogen masers. Finally, although not a dominant factor, the state selector magnet design has also seen significant reduction in size and weight [30]. The improvement arises from using the stronger rare-earth magnets rather than the Alnico V magnets in earlier designs.

IV. Q-Enhanced Compact Hydrogen Maser Oscillator

For sustained maser oscillation, the power radiated by the atoms must be sufficient to overcome the losses in the microwave cavity. This requirement cannot be met by arbitrarily increasing the atomic flux due to spin-exchange collision relaxation which is proportional to the flux. Indeed, there is both a minimum and a maximum flux level beyond which the maser will not oscillate. The power output P in a maser oscillating at an angular frequency ω can be expressed in terms of a critical power P_c and a threshold flux I_{th} as [13]

$$\frac{P}{P_c} = -2q^2\left(\frac{I}{I_{th}}\right)^2 + \frac{(1-3q)I}{I_{th}} - 1$$

where

$$P_c = \frac{1}{2} I_{th}\hbar\omega$$

$$I_{th} = \frac{\hbar V_b}{4\pi\mu_0^2\eta' Q T_t^2}.$$

Here I is the flux of atoms in the upper level of the maser transition. The quality factor q is defined by

$$q = \frac{\hbar\sigma v_r}{8\pi\mu_0^2}\frac{T_b}{T_t}\frac{1}{\eta' Q}\frac{I_t}{I}.$$

V_b is the volume of the storage bulb, $\hbar$ is Planck's constant divided by 2π, μ_0 is the magnetic moment of the atom, Q is the effective cavity Q, σ is the spin-exchange collision cross section, v_r is the relative velocity between colliding atoms, T_b is the time constant of the storage bulb, T_t is the total density-independent relaxation time, and I_t is the total atomic flux. The filling factor η' provides a measure of the coupling between the radiating atoms and the cavity elec-

tromagnetic field and is defined by

$$\eta' = \frac{\langle H_z \rangle_b^2}{\langle H^2 \rangle_c} \frac{V_b}{V_c}.$$

The atomic radiation is stimulated by the axial component of the microwave magnetic field H_z and $\langle H_z \rangle_b$ is its average over the storage bulb. $\langle H^2 \rangle_c$ is the square of the microwave magnetic field averaged over the volume V_c of the cavity and is thus proportional to the energy stored in the cavity.

To meet the condition that both P and I be positive quantities, the quality factor q must be less than 0.172 [13]. This condition for maser oscillation is due to spin-exchange collisions. If we neglect spin-exchange collision relaxation (i.e., letting $\sigma = 0$), the expression for the maser power output can be rewritten as

$$P = \frac{1}{2} \hbar\omega(I - I_{th})$$

which shows the physical meaning of the threshold flux I_{th}.

In a compact maser, the increased wall collision relaxation and the small $\eta'Q$ product due to the low intrinsic Q of the compact cavity make it difficult to satisfy the oscillation condition $q < 0.172$. Nevertheless, there is a good case for an oscillating compact maser. A maser oscillator provides a superior signal-to-noise ratio, which is a prerequisite for good short-term stability. Since oscillation occurs at the atomic resonant frequency where the atomic medium provides the maximum gain, possible systematic errors in high-precision line center determination due to electronic circuits are greatly reduced [31]. Finally, assuming that the cavity frequency is held constant, an oscillating maser is expected to have better stability than a similar maser operating as a narrow bandpass amplifier below the threshold for oscillation [32]. The approach adopted by workers at Hughes Research Laboratories is to enhance the Q of an electrode-loaded cavity by positive feedback. In this case, in contrast to traditional maser designs where the cavity is a relatively isolated component, the coupling network is an essential part of the cavity resonant system. To overcome the sensitivity of the Q-enhanced cavity frequency to external perturbations, an electronic cavity stabilization servo system is an integral part of the receiver design.

A schematic of Hughes' Q-enhanced maser oscillator is shown in Fig. 3. The signal processing electronics can be divided into three parts. The Q-enhancement loop (consisting of the microwave amplifier, a phase shifter, and an attenuator) couples a portion of the amplified maser signal back into the cavity. If the input and output cavity coupling coefficients are β_1 and β_2, and if there is no net transmission phase shift in the feedback loop, the enhanced cavity Q, Q_e, is [33]

$$Q_e = \frac{Q_0}{1 + \beta_1 + \beta_2 - 2G\sqrt{\beta_1\beta_2}}$$

where Q_0 is the unloaded Q of the cavity and G is the loop amplitude gain which determines the degree of Q enhancement. Typically, a subcompact maser employing a 7.5-cm-diameter electrode loaded cavity requires an enhancement factor of about 8, given a loaded cavity Q_e of 40 000 or an $\eta'Q_e$ product of 20 000.

A coherent heterodyne receiver processes the maser oscillation signal to phase-lock a slave VCXO. This portion of the receiver is similar to that for a conventional maser. The VCXO provides the system output as well as reference for the local oscillators of the receiver. The system output frequency is adjustable by means of a high-resolution synthesizer.

An important part of the receiver is the cavity stabilization servo system [34]. The system operates by alternately injecting sideband test signals at the half-power response frequencies of the cavity. The signals are generated by upconverting the 20.4-MHz output of a square wave modulated synthesizer with the 1.4-GHz local oscillator to alternately generate the two sideband frequencies. After transmission through the cavity and subsequent downconversion, the rectified test signals are synchronously detected. Any inequality in the test signals is used to drive an integrator whose output is used to bias a varactor reactance tuning diode to force the transmitted sideband test signals to equality. A feature of the cavity servo is that the cavity can

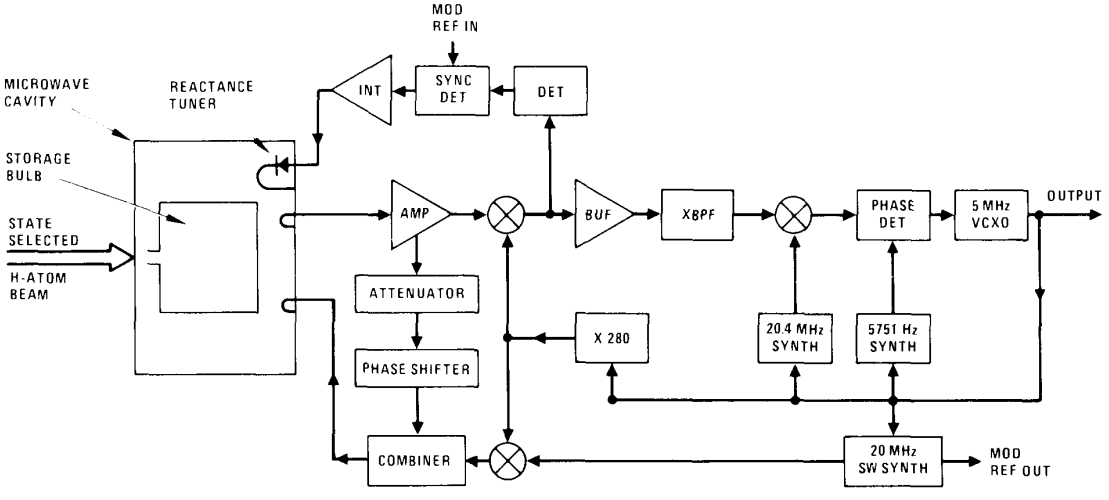

Fig. 3. Schematic of Hughes Q-enhanced maser oscillator.

be controlled at any desired frequency. This allows the maser to operate at the spin-exchange tuned cavity frequency where the maser output frequency is independent of flux variations. Spin-exchange tuning improves maser stability and also serves as an important diagnostic tool.

The feedback compresses the thermal noise distributed over the wider intrinsic response range of the cavity into the narrower spectral response range of the Q-enhanced cavity. The phase-perturbing effect of the noise power in the cavity ultimately limits the stability of the maser. This can be seen in the expression for the stability of the Q-enhanced maser oscillator given by [33]

$$\sigma^2(\tau) = \frac{kT}{2Q_a^2 P\tau}\frac{Q_e}{Q_0}\left[(1 + \beta_1 + \beta_2) + \frac{N-1}{4\beta_2}\left(1 + \beta_1 + \beta_2 - \frac{Q_0}{Q_e}\right)^2\right]$$

where $\sigma^2(\tau)$ is the two-sample variance, or Allan variance, Q_a is the atomic line Q, k is Boltzmann's contant, N is the noise figure of the first amplifier, T is the cavity and amplifier temperature, and τ is the measurement interval. The first term shows the detrimental effect of the Q enhancement where the variance is directly proportional to the enhancement factor Q_e/Q_0. The second term is the contribution from the noise of the amplifier. Improvements in both the intrinsic cavity Q and the amplifier noise figure will lead to improved maser stability. Due to the quadratic dependence of the maser power output on the flux, theory predicts an optimal operating flux as well as an optimal Q_e.

Several oscillating compact and subcompact masers, including an engineering model for space-borne applications, have been built at Hughes [35]. The masers were fabricated in three progressively smaller sizes, each size being determined mainly by the dimensions of the electrode-loaded microwave cavity (Table 2). CHYMNS-I and -II are proof-of-principle experimental masers. As the name implies, the EDM (engineering development model) space maser is a space-compatible design with telemetry interface for complete control and monitoring of the maser operation. The maser has successfully passed shake and vibration tests at the qualification level and is currently undergoing thermal vacuum tests. CHYMNS-IIIb is a prototype manually operated subcompact maser. CHYMNS-III-1 employs the same physics package as CHYMNS-IIIb, but is more user friendly. Its microprocessor-controlled operation includes automatic startup, monitoring of operating parameters, and an IEEE-488 computer interface. The volumes of the physics units range from approximately 65.5 l (4000 in^3) for the experimental maser CHYMNS-I to 8.8 l (542 in^3) for the newer subcompact maser CHYMNS-III. The latter weighs 10.2 kg (22.5 lb) and is probably the smallest hydrogen maser in the world at the present time. The physics unit of a CHYMNS-III subcompact maser, with the outer cover removed, is shown in Fig. 4. The small size of CHYMNS-III makes it practical to house the physics unit and the front-end microwave electronics in a hermetically sealed isothermal enclosure. Thermoelectric coolers are used for bidirectional temperature control of this outer cover, assuring a stable operating environment for the most sensitive components of the maser over a wide range of ambient conditions. The masers have comparable electronics-limited long-term stability performance since they all employ the same basic electronic design. That characteristic makes the approximately 30% sacrifice in short-term stability for each threefold reduction in the volume of the device a very favorable trade-off. However, further size reduction will bring diminishing returns due to the lower Q of the smaller cavities, the higher wall collision relaxation associated with smaller storage bulbs, and the fact that the cavity will constitute a smaller fraction of the total device volume.

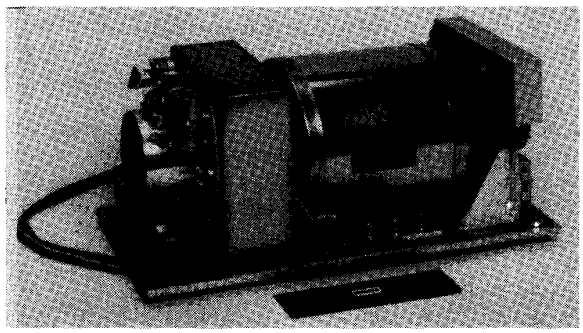

Fig. 4. Physics unit of CHYMNS-III subcompact hydrogen maser (with outer cover removed).

A. Stability of Oscillating Compact Masers

The stability of the oscillating compact hydrogen masers has been evaluated by comparing the masers against each

Table 2 Characteristics of Oscillating Compact Hydrogen Masers

	CHYMNS-I	CHYMNS-II	EDM Space Maser	CHYMNS-IIIb	CHYMNS-III-1
Cavity dimension $D \times L$ (cm)	15.2 × 15.2	10.4 × 15.2	10.7 × 15.8	7.6 × 7.6	7.6 × 7.6
Physics unit volume (l)	65.5	22.1	28.5	8.8	8.8
System dimension (cm)	Experimental	Experimental	21.8 × 21.8 × 59.7 10.7 × 32.8 × 39.1	17.8 × 30.5 × 43.2	26.0 × 61.0 × 43.2
Weight (kg)			29.1	19.5	40.0
Power consumption (W)			64	63	100
σ_{theory}*	1.9×10^{-14}	3.1×10^{-14}	3.1×10^{-14}	3.9×10^{-14}	3.9×10^{-14}
$\sigma_{measured}$*	2.4	3.0	6.9	4.1	4.1

*τ = 400 s.

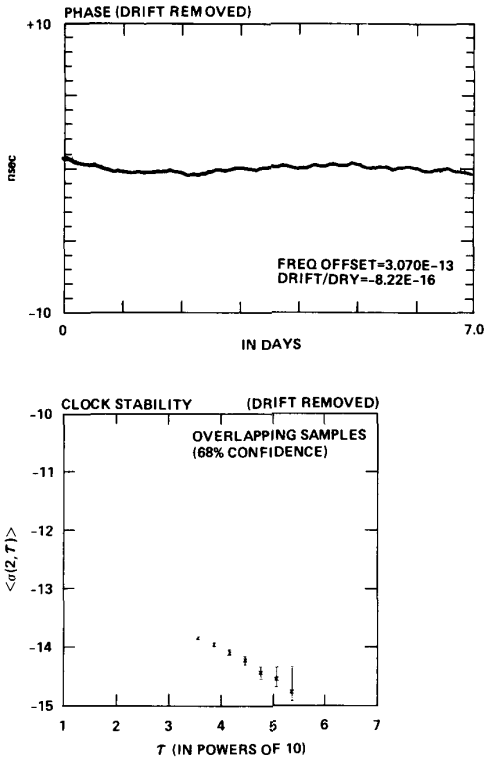

Fig. 5. Comparison of CHYMNS-IIIb versus CHYMNS-I.

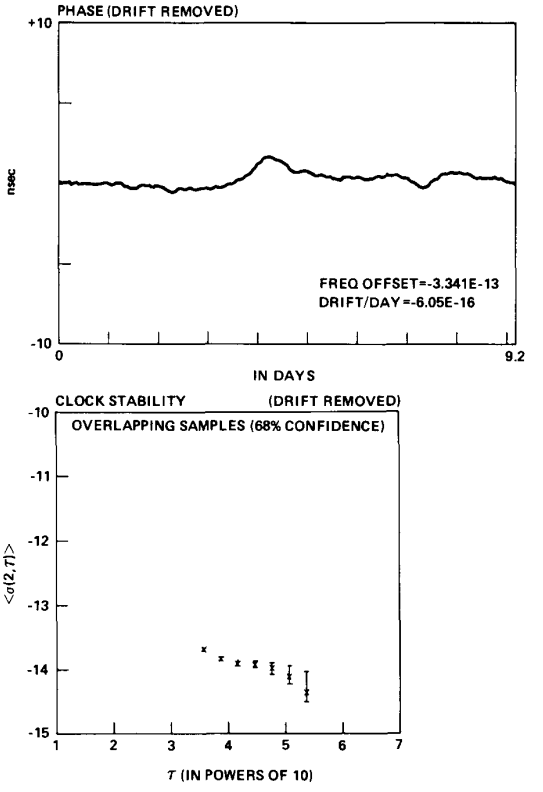

Fig. 6. Comparison of CHYMNS-II versus CHYMNS-I.

other as well as against a full-size hydrogen maser. A frequency stability measurement system capable of testing multiple standards simultaneously (with provisions for evaluating short-, medium-, and long-term stability performance) developed by workers at NRL has been used at Hughes. A stability comparison of the subcompact maser CHYMNS-IIIb versus CHYMNS-I is shown in Fig. 5. The fitted drift rate of several parts in 10^{-16} per day is generally obtained in a comparison between two oscillating compact masers in a relatively constant environment. Sudden temperature and humidity changes have detrimental effects on the stability of the masers. The effect of ambient variations can be seen, in both the phase data and the root Allan variance plot, in a comparison of the unpackaged experimental compact masers CHYMNS-I versus CHYMNS-II shown in Fig. 6. All these data were taken in normal laboratory environment without any special environmental controls. The importance of the operating environment can be seen from the data shown in Fig. 7. The data were taken during thermal vacuum tests of the EDM space maser [23]. The stability of the maser was monitored using the VLG11 P10 full-size maser as the reference. During the run, the temperature of the baseplate (temperature profile shown in insert) on which the maser was mounted was raised from 30 to 37°C. No measurable frequency change was observed. In another experiment, a 10°C, 12-h-period sinusoidal temperature modulation was applied to the baseplate. Again, no correlated frequency variation due to the thermal modulation was observed. The low sensitivity of the maser to temperature variations in a vacuum environment is aided by the absence of humidity. Humidity variations have sig-

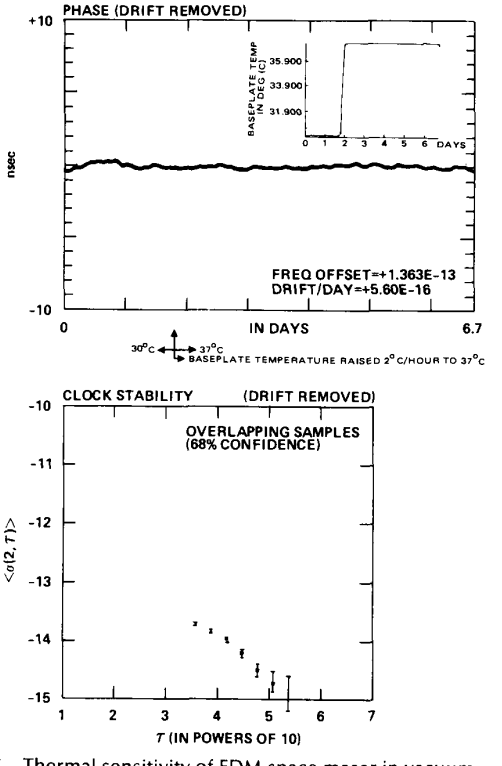

Fig. 7. Thermal sensitivity of EDM space maser in vacuum chamber. A 7°C temperature step (insert) produced no observable frequency change.

nificant effects on the operation of electronic circuits. Since all atomic clocks operate with very low level atomic resonant signals and rely on electronic circuits for signal conditioning, the consequent perturbation on the stability of atomic clocks is getting increasing attention [36].

Long-term stability measurement of a hydrogen maser is usually constrained by the lack of a superior standard, preferably more than one to minimize ambiguities, for comparison. GPS is beginning to provide some relief. Time transfer via GPS is a powerful tool for comparing remotely located clocks. In the common-view technique [9], two receivers, each phase-locked to one of the clocks to be compared, track the transmission from a given satellite simultaneously. The satellite-borne clock is used as a transfer standard. When one set of tracking data is subtracted from the other, we obtain a comparison between the two remotely located clocks. At a given location, the satellites in the current developmental GPS configuration are visible only for a few hours a day. This limits the common-view data collectible each day. The fluctuations in the tracking data for each sidereal day are significantly higher than the subnanosecond fluctuations in a comparison between two local maser clocks. However, over longer intervals, significant systematic variations between the clocks can be determined. A comparison of CHYMNS-II located at Hughes Research Laboratories in Malibu, CA, versus MC-USNO, the master clock at the U.S. Naval Observatory in Washington, DC, via the GPS common-view technique is shown in Fig. 8. The glitch near the middle of the plot was caused by a building air-conditioning failure which lasted approximately 32 hours and caused the room temperature to drop from a normal value of about 22°C to as low as 13°C. The cavity servo system in the unpackaged CHYMNS-II experimental maser was unable to compensate for this abnormal temperature variation. The saturation of the servo integrator produced a free-running condition, resulting in a relatively large maser frequency shift. However, the maser frequency recovered to about 1×10^{-14} after the normal ambient conditions were restored. After subtracting a constant offset of 1.22×10^{-13} (residue plot) and without any smoothing, the 35-day tracking data showed a standard phase deviation of 6.91×10^{-9} s and a standard frequency deviation for the daily tracking data of 9.95×10^{-14}. The fitted drift rate of -8.55×10^{-16} per day is consistent with the local comparisons between oscillating compact masers. Note that the standard frequency deviation for the daily tracking data given is much higher than that for the individual standards employed in the comparison, and the number is also not a fair reflection of the capability of the GPS common-view technique. As shown by Weiss and Allan [37], signal processing incorporating statistical smoothing and filtering of the tracking data is essential for obtaining the most from the satellite-based time transfer technique.

B. Another Implementation of Q-Enhanced Maser

To minimize the sensitivity of the Q-enhanced cavity frequency to external perturbations, Peters has employed a transistor amplifier coupled directly to the cavity. No component involved in cavity Q enhancement is located beyond

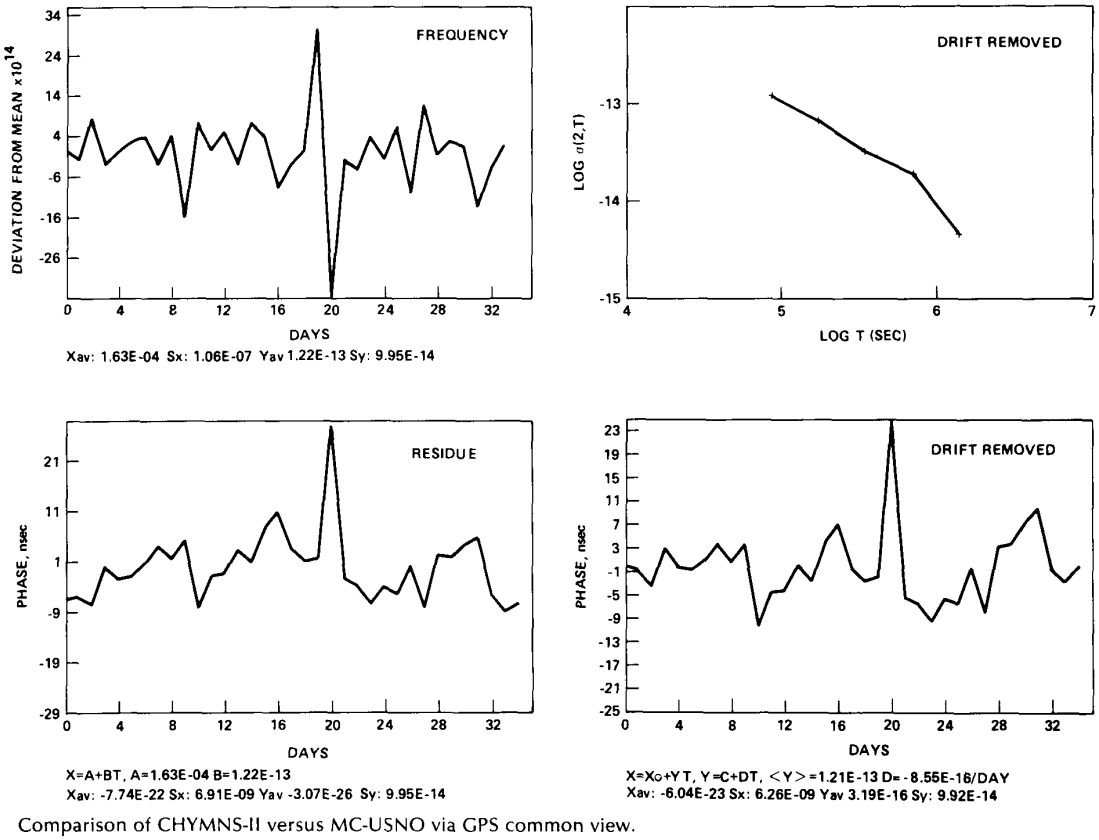

Fig. 8. Comparison of CHYMNS-II versus MC-USNO via GPS common view.

the immediate vicinity of the controlled environment of the maser cavity [38]. The phase and gain parameters are adjusted by varying the transistor bias voltage. Reducing the number of components and the elimination of cavity coupling transmission lines are desirable results of the approach. However, to optimize the performance of a Q-enhanced maser, it is necessary to be able to adjust the gain and phase parameters independently. Not enough data are available to demonstrate the effectiveness of this approach.

V. Passive Compact Hydrogen Maser

An alternate approach to a compact hydrogen maser frequency standard or clock is to use the stored hydrogen atoms as a narrow-bandpass amplifier [24], [25]. A resonant test signal synthesized from the slave VCXO is injected into the cavity. The narrow resonant linewidth and excellent signal-to-noise ratio (SNR) of the maser provide very sensitive frequency discrimination. The transmitted test signal is detected for amplitude and phase deviations caused by interaction with the stored atoms. The error signal is used to regulate the slave VCXO, closing the frequency control loop. The attractiveness of the approach is that there is no oscillation condition to meet. Therefore a high-Q cavity is not essential. Since cavity drift pulling of the maser output frequency is proportional to the cavity Q, using a low-Q cavity gives correspondingly low sensitivity to cavity drift. For a given cavity drift rate, the contribution of the cavity to the long-term stability of the maser should be improved compared to that in an oscillating maser. On the other hand, if we consider the cavity as a filter of thermal noise, a low-Q cavity will provide correspondingly low selectivity. Analysis has shown that using an oscillating maser provides better short-term stability than operating the maser passively by reducing its cavity Q to just below the threshold for oscillation [32].

Passive compact hydrogen masers have been developed by workers at NIST (formerly NBS) [25]. The cavity design employs dielectric loading, thus the size of the cavity remains the same through several iterations of the passive compact masers. The cavity is fabricated from a 14.5-cm-OD right circular cylinder of low-loss Al_2O_3 ceramic. A 10.5-cm-diameter by 13.6-cm-long bore down the axis of the cylinder coated with FEP 120 Teflon forms an integral storage bulb. The conducting envelope is formed by several layers of silver paint coating the outside of the cylinder. The unloaded Q of the cavity lies between 5500 and 6700. The cavity also forms part of the maser vacuum envelope, resulting in additional size reduction compared to the normal design. The complete maser is contained in a rack-mountable package measuring 26.7 × 66 × 45.5 cm and weighs 30 kg.

A schematic of the NBS passive maser is given in Fig. 9. A dual-modulation scheme is employed to lock both the system output VCXO (probe source) and the microwave cavity to the hydrogen resonance. A synthesized local oscillator is phase modulated at two frequencies, f_1 and f_2, before being injected into the microwave cavity containing the state-selected hydrogen atoms. The transmitted signal is envelope detected and processed in two synchronous detectors referenced to the respective modulation frequencies. f_1 nominally corresponds to the half-power bandwidth of the cavity. The error signal at f_1 is used to correct

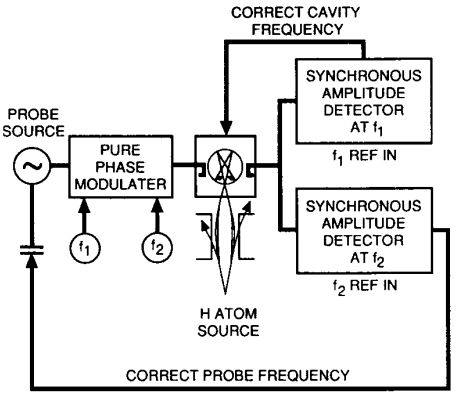

Fig. 9. Schematic of NBS passive maser.

the cavity frequency. f_2 nominally corresponds to the half-linewidth of the atomic resonance. The error signal at f_2 is used to correct the frequency of the VCXO. The cavity stabilization technique controls the cavity at the atomic resonance frequency without using an additional frequency synthesizer. The maser output will be sensitive to flux variations through spin exchange shift. A flux control feedback is employed to reduce the effect of this perturbation.

The reported stability of the passive compact maser is typically given by

$$\sigma_y(\tau) = 1.5 \times 10^{-12}\,\tau^{-1/2}, \qquad 1\ \text{s} < \tau < 10^5\ \text{s}.$$

Beyond one day, the stability is limited by environmental factors such as temperature and humidity. The reported drift rates, depending on the reference standard and the data segments, vary from 2 ± 5 to 9×10^{-16} per day.

VI. Conclusions

The development of compact, transportable, high-performance hydrogen masers has made significant progress during the last several years. Superior stability performance has been demonstrated in both the subcompact Q-enhanced maser oscillator and the passive compact hydrogen masers. The stability performance can be expected to improve from improved packaging to minimize environmental sensitivity and technological advancement in low-noise electronic components.

Material and technology advancement will impact the way we build masers. For example, it is conceivable that an electrode-loaded compact cavity of sufficiently high Q can be built using the new high-temperature superconductors. This will alleviate the need for cavity Q enhancement and reduce the effective noise temperature of the cavity. The perfect flux exclusion of the superconducting cavity eliminates the need for the multilayer external magnetic shields in the present designs, producing significant size and weight savings. The efficiency of a recirculating state-selected hydrogen atom source using superconducting magnets has already been demonstrated [39]. All these may be attained at liquid nitrogen temperatures or higher without the complexity of liquid helium cryogenics.

High-performance standards can also be expected from

technologies currently under development in various laboratories. A trapped mercury ion standard is already operational [40]. An optically pumped cesium-beam standard using laser radiation has been demonstrated [41]. Indeed, the application of laser-atom interaction promises an array of possibilities from population inversion by optical pumping to cooling and trapping of neutral atoms as well as ions to generate the desired extended interaction time between the atomic species and the resonant radiation field for superior frequency standard applications.

Acknowledgment

The author recognizes his inability to cite all recent contributions in the subject area. He regrets any omissions. He also wishes to thank Dr. R. L. Abrams for useful suggestions and Dr. R. R. Hayes for many fruitful discussions.

References

[1] P. A. Clements, S. E. Borutzski, and A. Kirk, "Maintenance of time and frequency in the JPL's DSN using the GPS," in *Proc. 16th Ann. Precise Time and Time Interval (PTTI) Application and Planning Meeting* (1984), pp. 427-446.

[2] G. M. R. Winkler, "Changes at USNO in global timekeeping," *Proc. IEEE*, vol. 74, pp. 151-155, 1986.

[3] R. Coates, J. Ryan, and T. Herring, "Time and frequency stability for the crustal dynamic project," in *Proc. 12th Ann. PTTI* (1980), pp. 649-662; K. I. Kellermann and A. R. Thompson, "The very long baseline array," *Science*, vol. 229, no. 4709, pp. 123-130, 1985.

[4] R. L. Beard, J. Murray, and J. D. White, "GPS clock technology and the Navy PTTI programs at the U.S. Naval Research Laboratory," in *Proc. 18th Ann. PTTI* (1986), pp. 37-53.

[5] B. W. Parkinson and S. W. Gilbert, "Navstar: Global Positioning System—ten years later," *Proc. IEEE*, vol. 71, pp. 1177-1186, 1983.

[6] D. W. Allan and H. Hellwig, "Time deviation and the prediction error for clock specification, characterization, and application," in *Proc. Position Location and Navigation Symp.* (1978), p. 29.

[7] T. B. McCaskill, J. A. Buisson, and S. B. Stebbins, "On orbit frequency stability analysis of the GPS Navstar's 3 and 4 rubidium clocks and Navstar's 5 and 6 cesium clocks," in *Proc. 15th Ann. PTTI* (1983), pp. 171-209; M. J. Van Melle, "Rubidium and cesium frequency standards status and performance on the GPS program," in *Proc. 18th Ann. PTTI* (1986), pp. 227-236.

[8] W. J. Klepczynski, "Modern navigation systems and their relation to timekeeping," *Proc. IEEE*, vol. 71, pp. 1193-1198, 1983; "Time transfer techniques: historical overview, current practices and future capabilities," in *Proc. 16th Ann. PTTI* (1984), pp. 385-402.

[9] D. W. Allan *et al.*, "Accuracy of international time and frequency comparison via Global Positioning System satellites in common view," *IEEE Trans. Instrum. Meas.*, vol. IM-34, pp. 118-125, June 1985.

[10] T. A. Stansell, Jr., "Civil GPS from a future perspective," *Proc. IEEE*, vol. 71, pp. 1187-1192, 1983.

[11] G. Missout, "PTTI applications in power utilities," in *Proc. 18th Ann. PTTI* (1986), pp. 491-502.

[12] D. Kleppner, H. M. Goldenberg, and N. F. Ramsey, "The theory of the hydrogen maser," *Phys. Rev.*, vol. 126, pp. 603-615, 1962.

[13] D. Kleppner *et al.*, "Hydrogen maser principles and techniques," *Phys. Rev.*, vol. A138, pp. 972-983, 1965.

[14] Y. M. Cheng *et al.*, "Hydrogen maser wall shift experiments and determination of the unperturbed hyperfine frequency of the ground state of the hydrogen atom," *IEEE Trans. Instrum. Meas.*, vol. IM-29, pp. 316-319, 1980.

[15] N. F. Ramsey, *Molecular Beams*. London, England: Oxford, 1956.

[16] H. Peters *et al.*, "Hydrogen masers for radio astronomy," in *Proc. 41st Ann. Freq. Contr. Symp.* (1987), pp. 75-81; T. K. Tucker and G. J. Dick, "Performance of a hydrogen maser with auto-tuning utilizing cavity Q modulation," *ibid.*, pp. 87-90.

[17] S. B. Crampton, "Spin-exchange shifts in the hydrogen maser," *Phys. Rev.*, vol. 158, pp. 57-61, 1967.

[18] S. B. Crampton, E. C. Fleri, and H. T. M. Wang, "Effects of atomic resonance broadening mechanisms on atomic hydrogen maser long-term frequency stability," *Metrologia*, vol. 13, pp. 131-135, 1977.

[19] S. B. Crampton and H. T. M. Wang, "Duration of hydrogen atom spin-exchange collisions," *Phys. Rev.*, vol. A12, pp. 1305-1312, 1975.

[20] H. E. Peters, "Small, very small and extremely small hydrogen masers," in *Proc. 32nd Ann. Frequency Control Symp.* (1978), pp. 469-475.

[21] H. T. M. Wang, J. B. Lewis, and S. B. Crampton, "Compact cavity for hydrogen frequency standards," in *Proc. 33rd Ann. Frequency Control Symp.* (1979), pp. 536-541.

[22] R. R. Hayes and H. T. M. Wang, "A subcompact Q-enhanced active hydrogen maser," in *Proc. 18th PTTI* (1986), pp. 611-620.

[23] E. S. Richter, B. A. Bettencourt, H. T. M. Wang, and R. R. Hayes, "Design considerations and performance of a spaceborne hydrogen maser frequency standard," in *Proc. 20th PTTI* (1988), pp. 111-121.

[24] J. White, A. Frank, and V. Folen, "Passive maser development at NRL," in *Proc. 12th Ann. PTTI* (1980), pp. 495-504.

[25] F. L. Walls, "Characteristics and performance of miniature NBS passive hydrogen masers," *IEEE Trans. Instrum. Meas.*, vol. IM-36, pp. 596-603, 1987.

[26] D. U. Gubser, S. A. Wolf, and J. E. Cox, "Shielding of longitudinal magnetic fields with thin, closely spaced, concentric cylinders of high permeability material," *Rev. Sci. Instr.*, vol. 50, pp. 751-756, 1979.

[27] J. White and K. McDonald, "Long term performance of VLG-11 masers," in *Proc. 35th Ann. Frequency Control Symp.* (1981), pp. 657-661.

[28] D. U. Gubser, S. A. Wolf, S. B. Jacoby, and L. D. Jones, "Magnetic shielding and vacuum test for passive hydrogen masers," in *Proc. 13th Ann. PTTI* (1981), pp. 791-799.

[29] H. T. M. Wang, "Application of metal hydrides for gas handling in hydrogen masers," in *Proc. 37th Ann. Frequency Control Symp.* (1983), pp. 7-11.

[30] H. E. Peters, "Magnetic state selection in atomic frequency and time standards," in *Proc. 13th Ann. PTTI* (1981), pp. 645-665.

[31] F. L. Walls, "Errors in determining the center of a resonance line using sinusoidal frequency (phase) modulation," *IEEE Trans. Ultrason., Ferroelec., Freq. Control*, vol. UFFC-34, pp. 592-597, 1987.

[32] C. Audoin, J. Viennet, and P. Lesage, "Hydrogen maser: active or passive?," *J. de Phys.*, colloque C8, vol. 42, pp. C8-159-170, 1981.

[33] P. Lesage and C. Audoin, "Frequency stability of an oscillating maser: analysis of the effect of an external feedback loop," *IEEE Trans. Instrum. Meas.*, vol. IM-30, pp. 182-186, 1983.

[34] H. T. M. Wang, "An oscillating compact hydrogen maser," in *Proc. 34th Ann. Frequency Control Symp.* (1980), pp. 364-369.

[35] H. T. M. Wang and R. R. Hayes, "Recent progress in oscillating compact hydrogen masers," in *Proc. 4th Symp. Frequency Standards and Metrology* (1988) (to be published).

[36] L. A. Breakiron, "The effect of ambient conditions on cesium clock rates," in *Proc. 19th Ann. PTTI* (1987), pp. 175-184; J. E. Gray, H. E. Machlan, and D. W. Allan, "The effect of humidity on commercial cesium beam atomic clocks," in *Proc. 42nd Ann. Frequency Control Symp.* (1988), pp. 514-518.

[37] M. A. Weiss and D. W. Allan, "An NBS calibration procedure for providing time and frequency at a remote site by weighting and smoothing of GPS common view data," *IEEE Trans. Instrum. Meas.*, vol. IM-36, pp. 572-578, 1987.

[38] H. E. Peters, "Experimental results of the light weight hydrogen maser development program," in *Proc. 36th Ann. Frequency Control Symp.* (1982), pp. 240-248.

[39] W. N. Hardy, M. D. Hurliman, and R. W. Cline, "Application of atomic hydrogen at low temperatures: the recirculating cryogenic hydrogen maser," in *Proc. 18th Int. Conf. on Low Temperature Physics* (1987), *Jpn. J. Appl. Phys.*, vol. 26, suppl. 26-3.
[40] L. S. Cutler, R. P. Giffard, P. J. Wheeler, and G. M. R. Winkler, "Initial operational experience with a mercury ion storage frequency standard," in *Proc. 41st Ann. Frequency Control Symp.* (1987), pp. 12-19.
[41] G. Theobald *et al.*, "Research on the optically pumped cesium beam frequency standards," in *Proc. 42nd Ann. Frequency Control Symp.* (1988), pp. 496-504.

Harry T. M. Wang was born on February 3, 1939, in Rangoon, Burma. He received the B.Sc. degree from the University of Rangoon in 1960 and the A.M. and Ph.D. degrees in physics from Harvard University, Cambridge, MA, in 1963 and 1967, respectively.

He joined Hughes Research Laboratories in 1975, where he leads the compact hydrogen maser development effort.

Dr. Wang is a member of the American Physical Society.